T-shaped molecular heat pump

Wei-Rong Zhong[1,2,*] and Bambi Hu[2,3]

[1]*Department of Physics and Siyuan Laboratory, College of Science and Engineering, Jinan University, Guangzhou 510632, China*

[2]*Department of Physics, Centre for Nonlinear Studies, and The Beijing-Hong Kong-Singapore Joint Centre for Nonlinear and Complex Systems (Hong Kong), Hong Kong Baptist University, Kowloon Tong, Hong Kong*

[3]*Department of Physics, University of Houston, Houston, Texas 77204-5005, USA*

(Received 18 September 2009; revised manuscript received 18 March 2010; published 3 May 2010)

We report on the first molecular device of heat pump modeled by a T-shape Frenkel-Kontorova lattice. The system is a three-terminal device with the important feature that the heat can be pumped from the low-temperature region to the high-temperature region through the third terminal. The pumping action is achieved by applying a stochastic external force that periodically modulates the atomic temperature. The temperature, the frequency, and the system size dependence of heat pump are briefly discussed.

DOI: 10.1103/PhysRevB.81.205401 PACS number(s): 44.10.+i, 05.60.−k, 44.05.+e, 63.20.−e

A heat pump is a machine or device that moves heat from a low-temperature heat source to a higher-temperature heat sink by applying an external work that modulates the environment of the system.[1] In the last decade, the nanoscale heat pump attracts more and more attentions due to its valuable applications.[2] Recent studies have carefully analyzed the physical mechanism of molecular heat pump through classical[3,4] and quantum[5–7] methods. Typically, in these schemes a carefully shaped external force[5] and a stochastic external force[6] periodically modulate the levels of the nano-object, leading to the pumping operation. This process has been confirmed theoretically to be available in a quantum Kubo oscillator. In classical systems a Brownian noise can lead to the reverse-direction movement of a molecular motor.[8,9] Therefore, it is also expected that stochastic external force can take heat continuously away from the cold heat bath and pump it into the hot heat bath.

In this paper, we build a classical prototype pumping device driven by stochastic external force (i.e., thermal noise or heat bath). In our model, as shown in Fig. 1(a), the first particle of two segments, H1, 2C, connects to two end of segment 1O2 via the junction 1 and 2, respectively. Segment OP and 1O2 are coupled via the midparticle of segment 1O2 and the first particle of segment OP. Each segment is a Frenkel-Kontorova (FK) lattice. The last particle of segment H1 and 2C are, respectively, connected to hot heat bath (high temperature, T_H) and cold heat bath (low temperature, T_C), while the last particle of segment OP is the control terminal.

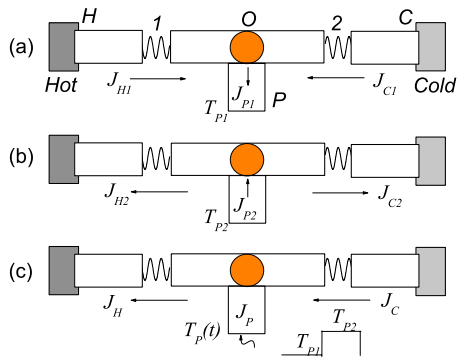

FIG. 1. (Color online) Configuration of the heat pump.

This T-shape FK model, which had ever been used to study thermal transistor[10] and thermal logic gate,[11] is similar to the experimental counterpart by putting a polymer chain or a nanowire on the top of adsorbed sheet.[12] Furthermore, a quasi-one-dimensional case of this model is the forked nanowire and nanotube, e.g., the T-shape nanowire[13] and Y-type carbon nanotube,[14] which stand by much potential experimental execution.

Segment H1 (2C) and 1O2 are coupled to 1 (2) via a spring of constant k_1 (k_2). Segments OP and 1O2, which are coupled via the midparticle of segment O with a spring of constant k_3, have the same parameters with the exception of the size. The number of the particles in segment 1O2 is nearly twice that in segment OP. The stochastic external force, which is here presented by a heat bath, is applied to modulate the last particle of OP segment. The temperature of the heat bath, $T_P(t)$, is a periodic square wave function. As shown in Fig. 1(c), $T_P(t)$ equals to T_{P1} in the first half period and T_{P2} in the second half period, respectively. The total Hamiltonian of the model is

$$H = \sum^{M} H_M + \sum H_{int} \tag{1}$$

and the Hamiltonian of each segment can be written as

$$H_M = \sum_{i=1}^{N_M} \left\{ \frac{p_{M,i}^2}{2m_M} + \frac{k_M}{2}(x_{M,i+1} - x_{M,i})^2 + \frac{V_M}{(2\pi)^2}[1 - \cos(2\pi x_{M,i})] \right\}, \tag{2}$$

where $x_{M,i}$ and $p_{M,i}$ denote the displacement from equilibrium position and the conjugate momentum of the ith particle in segment M, where M stands for H1, 1O2, 2C, or OP. N is the number of the particles in segments H1, 2C, and OP. The number of the particles in segment 1O2 is $2N+1$. $\Sigma H_{int} = H_1 + H_2 + H_3$, in which $H_1 = k_1(x_{H,1} - x_{O,1})^2/2$, $H_2 = k_2(x_{O,2N+1} - x_{C,1})^2/2$, and $H_3 = k_3(x_{O,N+1} - x_{P,1})^2/2$. We set the masses of all the particles be unit and use fixed boundaries, $x_{W,N+1} = 0$, where W stands for H, C, or P. The main parameters are $k_{H1} = 1.0$, $k_{2C} = 9.0$, $k_{1O2} = k_{OP} = 3.0$, $V_{H1} = 2.0$,

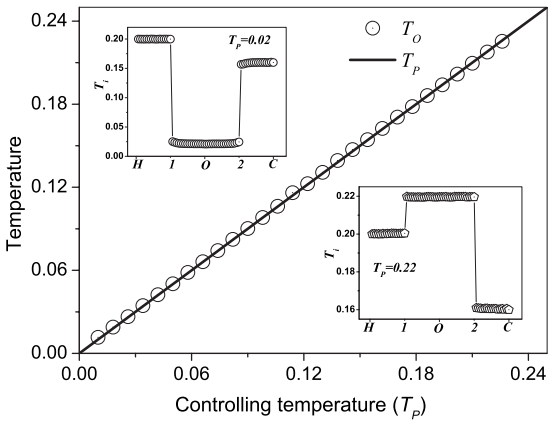

FIG. 2. Relationship between the temperature of particle O and the temperature of the controlling heat bath T_P. The inset is the temperature profiles along segments H-1-O-2-C as shown in Fig. 1(a) for T_P=0.02 and 0.22.

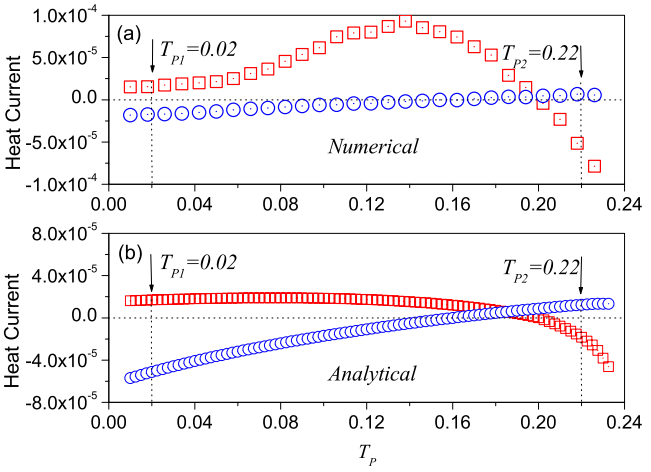

FIG. 3. (Color online) Heat currents through two terminals H (J_H, red square) and C (J_C, blue circle) versus the temperature of the controlling heat bath T_P. (a) Numerical results for the system size $4N+1=65$ and (b) analytical results based on Eq. (5).

$V_{2C}=4.5$, $V_{1O2}=V_{OP}=3.0$, $k_1=k_2=0.05$, $k_3=3.0$, $T_H=0.20$, and $T_C=0.16$.

In our simulations we use Nosé-Hoover thermostat[15] and integrate the equations of motion by using the fourth-order Runge-Kutta algorithm.[16] We have checked that our results do not depend on the particular thermostat realization (for example, Langevin thermostat). The local temperature is defined as $T_i=\langle p_i^2\rangle$, $\langle\ \rangle$ means time average. The local heat flux along the chain is defined as $J_{W,i}=k_M\langle p_i(x_i-x_{i-1})\rangle$, where W stands for H, C, and P. i is the order of the particle. The heat current, which flows from H to C(J_H), or O to C(J_C), or O to P(J_P), is defined as the positive current. The average kinetic energy is $E_K=\Sigma_{i=1}^{4N+1}\langle v_i^2\rangle/(4N+1)$, where v_i is the velocity of the ith particle and $4N+1$ is the system size, respectively. The simulations are performed long enough to allow the system to reach a steady state in which the local heat flux is constant along the chain.

Here the external perturbation has the same effect as a heat bath coupled to the particle in the end of segment OP. In our model, Fig. 2 shows the temperature of midparticle of segment 1O2, T_O, changes linearly with the temperature of the heat bath acted on segment P. Due to ballistic transport of weak link systems in low temperature,[17] the temperature of particle O nearly equals to the temperature of the heat bath $T_P(t)$, i.e., $T_O\approx T_P$. As the temperature of the heat bath connects to P is low enough, the temperature of interface particle O (T_O) is also small. Therefore, when T_O is smaller than T_H and T_C, the system absorbs energy from both heat baths and then the direction of the heat current is shown in Fig. 1(a), here we set the heat current $J_{H1}>0$, $J_{C1}<0$, and $J_{P1}>0$. When T_O is larger than T_H and T_C, the energy will dissipate from the system oscillator mode to heat baths and then the direction of the heat current is shown in Fig. 1(b), here the heat current $J_{H2}<0$, $J_{C2}>0$, and $J_{P2}<0$. The temperature profiles along the configuration of the system is shown in the inset of Fig. 2 for T_P=0.02 and 0.22. Actually, the temperature of the controlling heat bath is variable. Provided that we use the appropriate values of T_{P1} and T_{P2} and perform the simulation in long time enough (the simulation time is far larger than the relaxation time of the system), as shown in Fig. 1(c), we will get a negative value of the total heat current in one period, i.e., $J_H<0$ and $J_C<0$, which means a pumping operation.

This phenomenon can be understood from two essential physical principles: *negative differential thermal resistance (NDTR)* and *thermal rectification (TR)*.[10,11,17] These two effects produce nonlinear relationship between the heat current and the temperature difference. It can be explained in detail as follows.

As shown in Fig. 3(a), in the region of low temperature ($T_O<T_C<T_H$), when temperature T_O is decreased by decreasing the temperature of the controlling heat bath T_P, J_H increases first and then decreases to a small value, however, J_C decreases linearly. The dependence of J_H on the temperature difference T_H-T_O shows a NDTR effect. In high-temperature region ($T_O>T_H>T_C$), J_H and J_C have linear relationships with the temperature. In a brief, segment HO is in the open state for $T_O>T_H$ but in the close state for $T_O<T_H$. This effect is not visible in segment OC. If we select two appropriate values of T_P, T_{P1}=0.02 and T_{P2}=0.22, as the temperature in the first and the second half period, the total heat currents $J_H(J_{H1}+J_{H2})$ and $J_C(J_{C1}+J_{C2})$ equal to -4.30×10^{-5} and -1.15×10^{-5}, respectively. Heat pump works on the condition that the negative heat flux is larger than the positive one during a period.

The corresponding analytical method is also included. As reported in Refs. 18 and 19, we replace the first and second derivatives of the external potential by their thermal average with respect to the effective harmonic Hamiltonian, and then Eq. (2) can be approximated by self-consistent phonon theory as

$$\tilde{H}_M=\sum_{i=1}^{N_M}\left[\frac{p_{M,i}^2}{2}+\frac{k_M}{2}(q_{M,i+1}-q_{M,i})^2+\frac{g_M}{2}(q_{M,i})^2\right], \quad (3)$$

in which

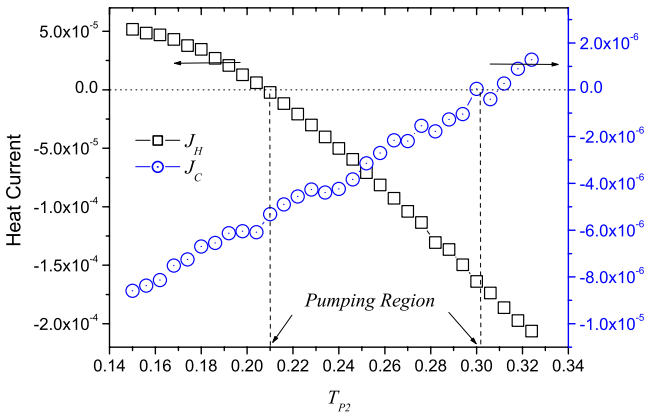

FIG. 4. (Color online) Temperature dependence of the heat current in a T-shape FK lattice. The vibration period of $T_P(t)$ is 5.0×10^6 steps and the system size is 65.

$$g_M = \frac{V_M}{2}\exp\left[-\frac{2\pi T_M}{\sqrt{g_M(4k_M+g_M)}}\right], \tag{4}$$

where T_M means the average temperature and M refers to segments HO, OC, and OP. Here we solve the transcendental Eq. (4) through calculating the intersection point of left part and right part of the equation.[20] As $k_1\to0$, considering classical Landauer-type equation, we can get the heat current flows from H to O as

$$J_H = \frac{k_B(T_H-T_O)}{2\pi}\int_{\omega_1}^{\omega_2}\chi(\omega)d\omega, \tag{5}$$

in which the transmission coefficient is

$$\chi(\omega)\approx\frac{k_1^2}{k_Hk_O}\sqrt{\frac{(4k_H+g_H-\omega^2)(4k_O+g_O-\omega^2)}{(\omega^2-g_H)(\omega^2-g_O)}}. \tag{6}$$

The cutoff frequencies range from $\omega_1=\max\{\sqrt{g_H},\sqrt{g_O}\}$ to $\omega_2=\min\{\sqrt{4k_H+g_H},\sqrt{4k_O+g_O}\}$, which correspond to the boundaries of the overlap band of left and right phonon spectra. Provided that T_H and T_O are available, then we can obtain the heat current flows from H to O, J_H. Similarly, as $k_2\to0$, we can also get the heat current from O to C, J_C. Due to the linear relationship of T_O and T_P, Fig. 3(b) analytically confirms the NDTR and TR effects in T-shape FK lattices, which is numerically presented in Fig. 3(a).

Heat pump is a dynamical and nonequilibrium effect during macroscopic time. Therefore, heat pump has some valid conditions. We give three main parameters which influence the state of heat pump significantly.

Temperature dependence. In order to obtain four heat currents, J_{H1}, J_{H2}, J_{C1}, and J_{C2}, shown in Figs. 1(a) and 1(b), obviously the temperature T_O should satisfy $T_O<T_C<T_H$ in the first half period and $T_C<T_H<T_O$ in the second half period, respectively. Since T_O almost equals to T_P, as illustrated in Fig. 2, T_P has to satisfy $T_P<T_C<T_H$ in the first half period and $T_C<T_H<T_P$ in the second half period, respectively. Here the main point is what is the range of $T_P(t)$. Generally, we fix the low-temperature level $T_{P1}(=0.02)$ and change the high-temperature level T_{P2}. Figure 4 displays that

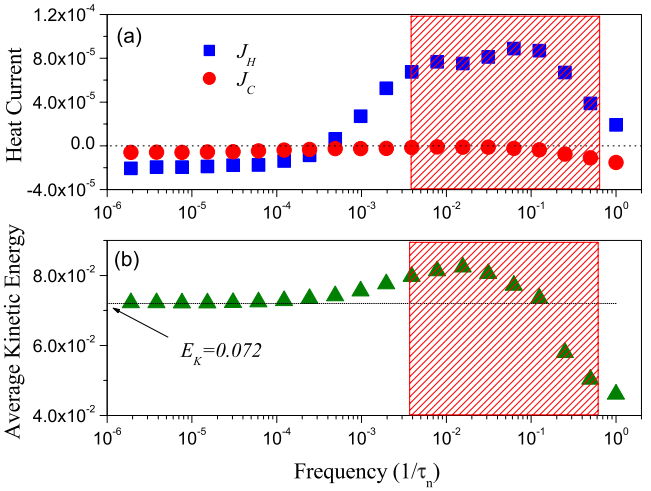

FIG. 5. (Color online) Frequency dependence of (a) heat currents and (b) average kinetic energy of heat pump. The remaining parameters are the same as for Fig. 4.

the total heat currents, J_H and J_C, are negative as T_{P2} ranges from 0.210 to 0.303. This range of T_{P2} is defined as pumping region. When $T_{P2}<0.210$ or $T_{P2}>0.303$, pumping effect cannot be realized. It is worth mentioning a point, where $T_{P2}=0.251$ and $J_H=J_C=-0.51\times10^{-5}<0$, indicates the optimum pumping.

Frequency dependence. In our simulation, the system relaxation time (τ_s) of our model is about 6.0×10^9 simulation steps, then $\tau_s=6.0\times10^7$. The oscillating frequency of single particle (ω_p or $1/\tau_p$) ranges from 2.5×10^{-3} to 6.2×10^{-1}, which can be calculated through the phonon spectral analysis of the particle's velocity.[10] In order to get a stable heat current, the vibration period of temperature level $T_P(t)$ should be far smaller than the system relaxation time. Furthermore, the vibration period of noise level cannot be near the oscillating period of single particle. As shown in Fig. 5(a), in the case of low frequency, the heat pump works normally with a stable negative heat current J_H. However, when the vibration frequency of temperature is increased to a value larger than 3.0×10^{-3}, the direction of heat current changes and the heat pump stops working. It is easily understood from the change in the average kinetic energy with the frequency. As shown in Fig. 5(b), the system maintains its average kinetic energy onto a value E_K $\{=\frac{1}{2}[E(T_{P1})+E(T_{P2})]=0.072\}$ at low frequency. However, the average kinetic energy has a significant change in the frequency region of single particle, which corresponds to the shadow area in Fig. 5. In this region, the frequency may match the oscillating frequency of single particle, the temperature of the controlling heat bath has a significant influence on the oscillating energy of every particle and the system is nonconservative. Therefore, we set the vibration period of temperature level, τ_n, be 5.0×10^4, which satisfies $\tau_p\ll\tau_n\ll\tau_s$.

System size effect. The results displayed above are for a system with $65(4N+1)$ particles. Since the heat pump mechanism in our model is due to the coupling between two asymmetric lattices it is reasonable to expect that the system size will definitely influence the heat pump efficiency. As shown in Fig. 6, the heat current is dependent on the system

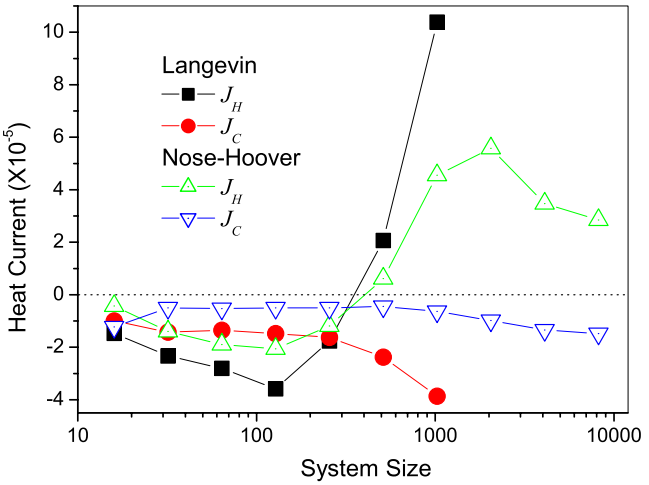

FIG. 6. (Color online) The finite-size effect of the pumping efficiency for two kinds of heat baths, Langevin (solid squares and circles) and Nosé-Hoover (open up triangles and down triangles). The remaining parameters are $T_{P1}=0.02$, $T_{P2}=0.22$, and $\tau_n=5.0\times10^4$.

size. The heat current of heat pump increases first and then decreases by increasing the number of particles. Finally, the heat pump stops working when the system size is larger than 500. This phenomenon can be understood by system size dependence of NDTR.[17] When the system size is increased, the system goes to completely diffusive transport regime and then NDTR disappears. Thus, the valid condition for heat pump will be unavailable.

We have to point out that in this paper we use the more complex four segments rather than three segments FK lattices just for the convenience of theoretical analysis. Actually, in the case of three segment lattices, the heat pump may work more efficiently. Finally, we would like to discuss the improvement of our heat pump model. Figure 1 displays a single heat pump working between two heat baths with small temperature difference. Moreover, this kind of single heat pump works with low pumping efficiency. Therefore, if we expect to get a more powerful heat pump, we can connect single heat pumps in series or in parallel.

Up to now we only pay attention to the behavior of the device as a heat pump, which requires $J_H<0$ and $J_C<0$; however, for the situation with only $J_C<0$ (when the system size is larger than 500 as shown in Fig. 6), which would be useful as a refrigerator mode to extract heat from the cold source, although in this case this heat will not go to the hot source but will go to the oscillating heat bath; anyway, the ensemble will globally act as a refrigerator.

In conclusions, we have reported the feasibility to produce molecular heat pump based on T-shape FK model. This device can pump the heat from the low-temperature region to the high-temperature region through controlling the atomic temperature of the third terminal. Although the heat pump presented here is only an ideal model, it can be easily imitated in experiment. The study may also be a valuable illumination in fabricating nanoscale heat pump. Besides, our heat pump model will help deeply understand the effect of negative differential thermal resistance.

We would like to thank members of the Centre for Nonlinear Studies for useful discussions. This work was supported in part by grants from the Jinan University Young Faculty Research Grant YFRG, the Hong Kong Research Grants Council RGC and the Hong Kong Baptist University Faculty Research Grant FRG.

*wrzhong@jnu.edu.cn

[1] *The Systems and Equipment Volume of the ASHRAE Handbook*, edited by M. Owen (ASHRAE, Atlanta, GA, 2004).
[2] A. Nitzan, Science **317**, 759 (2007).
[3] R. Marathe, A. M. Jayannavar, and A. Dhar, Phys. Rev. E **75**, 030103(R) (2007).
[4] N. Nakagawa and T. S. Komatsu, Europhys. Lett. **75**, 22 (2006).
[5] D. Segal and A. Nitzan, Phys. Rev. E **73**, 026109 (2006).
[6] D. Segal, Phys. Rev. Lett. **101**, 260601 (2008).
[7] Y. Wei, L. Wan, B. Wang, and J. Wang, Phys. Rev. B **70**, 045418 (2004).
[8] P. Hänggi and F. Marchesoni, Rev. Mod. Phys. **81**, 387 (2009).
[9] M. van den Broek and C. Van den Broeck, Phys. Rev. Lett. **100**, 130601 (2008).
[10] B. Li, L. Wang, and G. Casati, Appl. Phys. Lett. **88**, 143501 (2006).
[11] L. Wang and B. W. Li, Phys. Rev. Lett. **99**, 177208 (2007).
[12] V. Pouthier, J. C. Light, and C. Giraredet, J. Chem. Phys. **114**, 4955 (2001).
[13] Z. L. Wang, Z. W. Pan, and Z. R. Dai, Microsc. Microanal. **8**, 467 (2002).
[14] A. Cummings, M. Osman, D. Srivastava, and M. Menon, Phys. Rev. B **70**, 115405 (2004).
[15] S. Nosé, J. Chem. Phys. **81**, 511 (1984); W. G. Hoover, Phys. Rev. A **31**, 1695 (1985).
[16] W. H. Press, S. A. Teukolsky, W. T. Vetterling, and B. P. Flannery, *Numerical Recipes* (Cambridge University Press, Cambridge, 1992).
[17] W. R. Zhong, P. Yang, B. Q. Ai, Z. G. Shao, and B. Hu, Phys. Rev. E **79**, 050103 (2009).
[18] B. Hu, D. He, L. Yang, and Y. Zhang, Phys. Rev. E **74**, 060101 (2006).
[19] D. H. He, Ph.D. thesis, Hong Kong Baptist University, 2008.
[20] W. R. Zhong, Y. Z. Shao, and Z. H. He, Phys. Rev. E **74**, 011916 (2006).